

EXPERIMENTAL AND NUMERICAL INVESTIGATION OF PLANE AIR WALL JET: AN APPLICATION TO VERTICAL REFRIGERATED DISPLAY CABINETS

Fareed Hussain MANGI*, Asif Ali MEMON**, Jean MOUREH***

ABSTRACT

Design of an energy efficient air curtain in particularly vertical refrigerated display cabinet has become a new challenge. The classical air curtain in a closed circuit is a longitudinal jet of cold air blown through a nozzle and sucked back by a longitudinal recovery arrangement. For a better understanding of the dynamics of air curtains, complex and case specific geometries for a fully stocked refrigerated display cabinet can be reasonably simplified to that of a plane air wall jet. A jet is said to be a wall jet, if it is blown near a wall, Wall jet has immense applications in refrigerated display cabinets, Jet cutting, cooling through impingement, heat insulation, inlet devices in ventilation, separation control in airfoils and film cooling of turbine, heating, ventilation and air-conditioning and various industrial applications.

This study aims to develop an experimental prototype to study the interaction between plane air jet confining cavity and a transverse cross-flow. To validate the proper working of the experimentally developed prototype (especially energy efficient air curtain), in the first step an academic configuration was studied which is plane air wall jet, where analytical solutions and experimental measures are available. In the prototype as well as for the numerical investigation, the plane air wall jet was investigated by using two different nozzles of 4cm and 2cm widths respectively through whom air is blown by the blower at 5m/s from top to bottom on a rectangular two dimensional domain of $0.4 \times 0.5 \text{ m}^2$. The obtained experimental measurements, using Laser Doppler Velocimetry (LDV), are compared to numerical results obtained by the commercial CFD code Fluent using different turbulent models and correlations proposed in the literature for the mean velocity profiles, maximum velocity decay, flow entrainment, friction coefficient and turbulence properties.

1. INTRODUCTION

Refrigerated Display Cabinet (RDC) is used since long time with the purpose to display the refrigerated foodstuffs for selling to the public. RDCs are used in supermarkets, food stores, convenience stores and other places where refrigerated or deep frozen foodstuffs are sold. In a RDC, the products are cooled by means of cold air flowing along the product. Alternatively the product may be cooled by means of contact cooling through the shelf or surface on which the product is placed. A combination of both is also employed. An air curtain is a planar jet of air with large aspect ratio having higher momentum than its surrounding air, used to separate the refrigerated foodstuffs inside the Refrigerated display case from the outside warm air having different characteristics and properties like temperature, airborne particle, relative humidity, etc, in the store. Therefore the outside warm air does not have much influence on the refrigerated foodstuffs [8], [12]

and [13].

Air curtains are in use in many applications, i.e. Industrial climate control; air conditioned areas, industrial oven openings, dust and humidity control, mines, commercial entrances, cold storage (i.e. Refrigerated display cabinets), etc. Air curtains are often used in vertical directions and depending upon the application, they may be spilled through a circuit, or impinged on a surface located in the downstream of the jet. They may be isothermal or thermally conditioned depending upon the specific application [8].

The figure. 1 shows a classical air curtain view [5]. Here:

- H represents opening of the cabinet; and is longitudinal distance between nozzle outlet and mouth of recovery at suction mechanism;
- L_v represents longitudinal length corresponding to

*Laboratoire de Thermocinétique, CNRS-UMR 6607 Ecole Polytechnique - University of Nantes Rue Christian. Pauc, B.P. 50609, F-44306, Nantes cedex 3, France

**Energy and Environment Engineering Department, Quaid-e-Awam University of Engineering, Science and Technology, Nawabshah, Pakistan

***Genie des Procédés AN/Refrigeration Process Engineering (GPAN), Research Unit Cemagref Antony Paris France.

- the cabinet length;
- B defines width of nozzle at origin;
- V_l is the velocity at the origin in the axis of air curtain;
- $M&l$ represents the mass flow rate of air at blower and recovery;
- t_l is its temperature and x_l is the title of fluid blown;
- Angle ' A ' is the direction i.e. horizontal, vertical or inclination of air curtain;
- t_a and x_a are the atmosphere of the store or shop;
- t_i and x_i are the internal atmosphere of the display Cabinet.

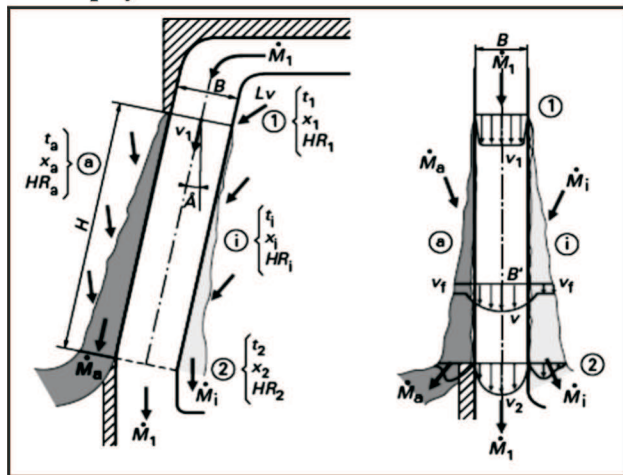


Figure 1: Air curtain (courtesy of Georges RIGOT (2009))

For a better understanding of the dynamics of air curtains, complex and case specific geometries for a fully stocked refrigerated display cabinet can be reasonably simplified to that of a plane air wall jet [4].

Jets are formed by the resultant differences of fluid pressure between two large fluid masses in the atmosphere or in confined places, particularly in the mid and upper levels. A jet is said to be a wall jet, if it is blown near a wall. In [11] a more formal definition of the wall jet given by Launder and Rodi (1981) is reported, "A shear flow directed along a wall where, by virtue of initially supplied momentum, at any station, the stream-wise velocity over some region within the shear flow exceeds that of the external stream". Because of diverse uses of plane turbulent wall jets in many

applications, e.g. Jet cutting, cooling through impingement, heat insulation, inlet devices in ventilation, separation control in airfoils and film cooling of turbine, heating ventilation and air-conditioning industrial applications, researchers are very keen to evaluate wall jets from many aspects like attempts to find scaling laws and correlations [1], [6], [15] and [16].

Many experimental studies on wall jets have been carried out by various researchers e.g. starting from Förthmann (1934) and then followed by Zerbe and Selna (1946), Tuve (1953), Sigalla (1958), Myers et al (1961), Schwarz and Cosart (1961), Sforza and Herbst (1970), Sforza (1977) and Awbi (1991), and by having a good observation on these studies the formation and behaviour of wall jet, as shown in figure. 2 [14].

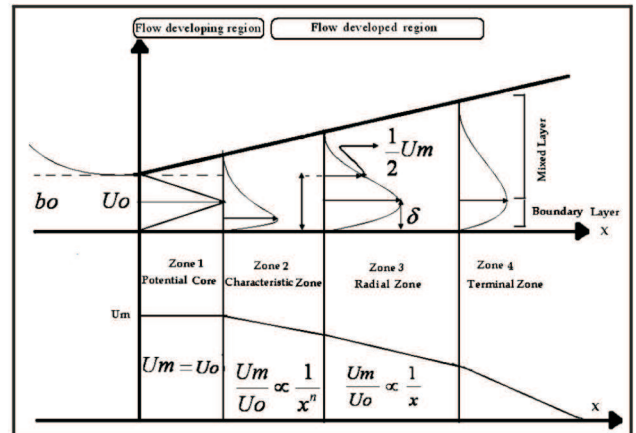


Figure 2: Characteristic Zones of Plane wall jet (courtesy of Tapsoba)

The plane wall jet can be divided into four zones in span-wise direction:

Zone 1 is called zone of potential core, here velocity remains constant in a conical and central part at the outlet of a jet. This implies that in this zone maximum velocity is equal to the velocity at inlet.

$$U_m = U_o \quad (1)$$

In zone 2, flow is developed in the perpendicular direction at the wall and can be distinguished in two layers [18] and [19]. The layer near the wall is known as boundary layer, and the layer formed on the side of air is known as mixed layer. In this zone, axial velocity decreases gradually according to the behaviour law:

$$\frac{U_m}{U_o} = \frac{1}{x^n} \quad (2)$$

Zone 3 is known as radial zone, because of its semi-circular velocity profile. This is characterized by a high turbulent flux, and the maximum velocity in this zone is inversely proportional to the axial distance:

$$\frac{U_m}{U_o} \propto \frac{1}{x} \quad (3)$$

Zone 4 is said to be terminal zone. It is a zone of rapid diffusion in which velocity is relatively weak and tends to zero. Wall jet growth is about 0.7 times that of the free jet [15]. There are also some empirical equations for the wall jet growth proposed in the literature [17].

This study aims to develop an experimental prototype to study the interaction between plane air jet confining cavity and a transverse cross-flow. To validate the proper working of the experimentally developed prototype (especially energy efficient air curtain), in the first step, an academic configuration was studied which is plane air wall jet, where analytical solutions and experimental measures are available. In the prototype as well as for the numerical investigation, the plane air wall jet was investigated by using two different nozzles of 4cm and 2cm widths respectively through whom air is blown by the blower at 5m/s from top to bottom on a rectangular two dimensional domain of 0.4x0.5m². The obtained experimental measurements, using Laser Doppler Velocimetry (LDV), are compared to numerical results obtained by the commercial CFD code Fluent using different turbulent models and correlations proposed in the literature for the mean velocity profiles, maximum velocity decay, flow entrainment, friction coefficient and turbulence properties. This paper is organized as follows: in the Section 2 experimental set up and problem description are described, Section 3 is devoted to discuss the results and discussions, Section 4 expresses the conclusion and future prospective.

2. EXPERIMENTAL SETUP AND PROBLEM DESCRIPTION

An overall view of the experimental set up is shown in Figure 3. This consists of a prototype made up of Plexiglas, usage of Plexiglas permits flow visualization of the physically studied domain and also it permits laser penetration to capture the seeded particles on the flow, a centrifugal blower through which air is blown

from the top to the bottom (i.e. vertically) of the prototype, an arrangement to accommodate the honeycombs and grills with different sizes of holes in a rectangular box through which turbulence intensity is minimized and a smooth, regular and less distribution of turbulence intensity at the nozzle exit is achieved, a nozzle with width of either 4cm or 2cm is installed vertically (as we are interested here in vertical top to down flow), the configuration which is adjustable for testing wall jet as well as cavity flow (this is made possible with a glass wall which can be adjusted according to our requirements) to analyse the air jet, and an air recovery system through which recirculation is made possible, an arrangement through which oil is stored to generate seeded particles during acquisitions, and also a flow meter apparatus is installed to check the inlet conditions (i.e. velocity and flow) before starting acquisition. Wall jet is obtained by placing a wall of glass at the nozzle exit as shown in figure 3, two types of nozzles having different width (i.e. 4cm and 2cm) were used to observe wall jet while air is blown vertically from top to bottom and it is sucked back and therefore it is re-circulated. All measurements are taken by using Laser Doppler velocimetry (LDV), with different positions on X and Y axis.

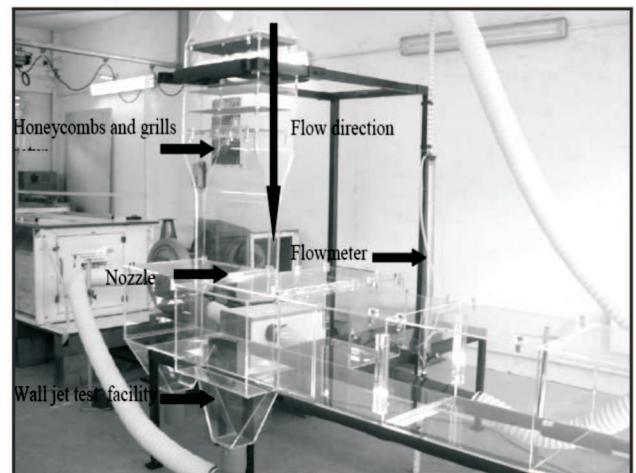


Figure 3: Prototype

2.1. GRILLS AND HONEYCOMBS ARRANGEMENT

An arrangement of grills and Honeycombs with different sizes of holes in a rectangular box is made before the nozzle inlet. Purpose of this arrangement is to reduce the turbulence intensity further more with this we may get a smooth, regular and less turbulent flow with minimum fluctuation of velocity at nozzle inlet. To select the better setup, various configurations of

different grills have diameters of holes 4.8mm, 3.2mm, 2.3mm, 1.7mm and 1.2mm and honeycombs having diameter of holes 3mm were tested to observe the turbulence intensities. The configurations were tested with measuring velocity profiles of wall jet with nozzle width of 2cm. Arrangements of grills and honeycombs in a rectangular box before nozzle inlet are given according to their placement from top to bottom in the table 1:

Table 1: Tested Configurations of Honeycombs and grills arrangement

SNo:	1 st Configuration	2 nd Configuration	3 rd Configuration	4 th Configuration	5 th Configuration
01	Honeycomb ($\phi=3\text{mm}$)	Honeycomb ($\phi=3\text{mm}$)	Grill ($\phi=1.2\text{mm}$)	Honeycomb ($\phi=3\text{mm}$)	Honeycomb ($\phi=3\text{mm}$)
02	Grill ($\phi=4.8\text{mm}$)	Honeycomb ($\phi=3\text{mm}$)	Honeycomb ($\phi=3\text{mm}$)	Honeycomb ($\phi=3\text{mm}$)	Grill ($\phi=4.8\text{mm}$)
03	Grill ($\phi=2.3\text{mm}$)	Grill ($\phi=3.2\text{mm}$)	Honeycomb ($\phi=3\text{mm}$)	Honeycomb ($\phi=3\text{mm}$)	Grill ($\phi=3.2\text{mm}$)
04	Grill ($\phi=1.7\text{mm}$)	Grill ($\phi=1.7\text{mm}$)	Grill ($\phi=2.3\text{mm}$)	Grill ($\phi=2.3\text{mm}$)	Grill ($\phi=2.3\text{mm}$)
05	Gill ($\phi=1.2\text{mm}$)	Gill ($\phi=1.2\text{mm}$)	Grill ($\phi=1.7\text{mm}$)	Grill ($\phi=1.7\text{mm}$)	Grill ($\phi=1.7\text{mm}$)

Comparisons of turbulent intensity obtained are shown in figure 4; the turbulence intensity changes with changing in placements of grills with different sizes of holes and honeycombs. As it is obvious entrainment is responsible for most of refrigerating load in display cases, so it is possible to decrease amount of entrainment in air curtain therefore one can design an air curtain which has less fluctuation in velocity thus less turbulence intensity, keeping in view this importance different arrangements of honeycombs and grills were checked by using Laser Doppler velocimetry (LDV).

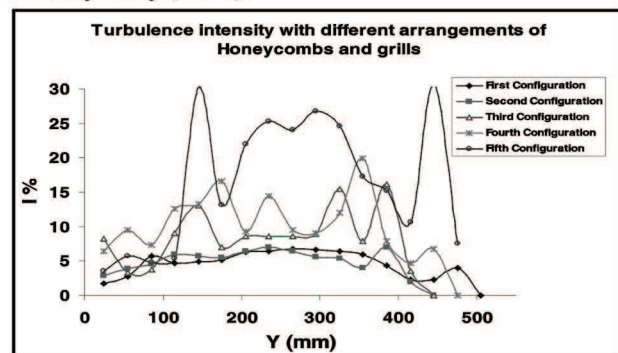


Figure 4: Turbulence intensity function of placement of honeycombs and grills

Figure 4, shows with first configuration the turbulence intensity obtained is fluctuating between 0% and 5%, but it is approximately constant between 200mm and 350mm along the y-positions. Second configuration represents turbulence intensity between 0% and 5%, and with this configuration it is observed that turbulence intensity fluctuate span wise along y-positions, while the other three configurations (i.e. 3rd, 4th and 5th) predict turbulence intensity above the limit (i.e. 10% which is affordable), Therefore configuration was selected for our experimental work.

3. RESULTS AND DISCUSSION

As described in earlier section, that 2D wall jet configurations with two different nozzles with width (b_0) of 4 cm and 2 cm respectively were analyzed. For 4 cm configuration we used two different types of meshes i.e. coarse mesh and fine mesh which are generated with the GAMBIT software. The commercial software FLUENT was used as solver. The coarse mesh simulations standard wall function was selected. While for the fine mesh enhanced wall treatment was used. To validate the numerical results using LDV in the prototype, nozzles of width (b_0) 4 cm and 2 cm respectively were used.

3.1 BOUNDARY CONDITIONS

To investigate numerically the configuration as shown in figure 5 the boundary conditions are defined according to the physical problem description. The right vertical and left vertical sides of $0.4 \times 0.5 \text{ m}^2$ domain are defined as walls.

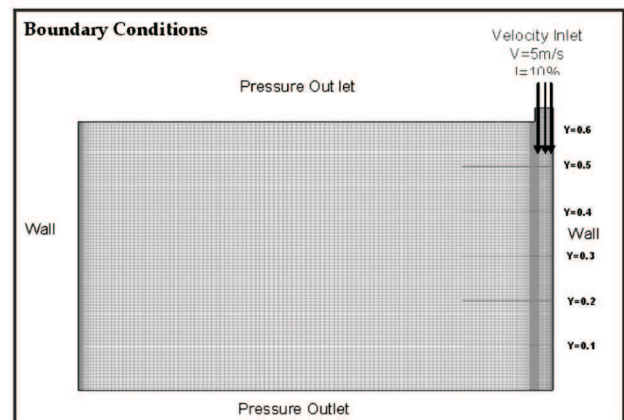


Figure 5: Boundary conditions in 2D wall jet configuration

As direction of jet is from top to bottom so some lines are marked to observe flow characteristics from flow developing region (i.e. Potential core) to the flow development region. To obtain free wall jet, upper and lower sides of the 2D configuration are considered as pressure outlets. To avoid recirculation and vortex formation, at the bottom near the jet and for the original nature of the jet, a very small pressure difference between two pressure outlets, which we have supposed here as $\Delta P=0.1$ Pa. Importance of this pressure difference is illustrated in figure 6 and 7.

In figure 6 with $\Delta P=0$, recirculation in the flow path lines observed which does not resemble the wall jet characteristics.

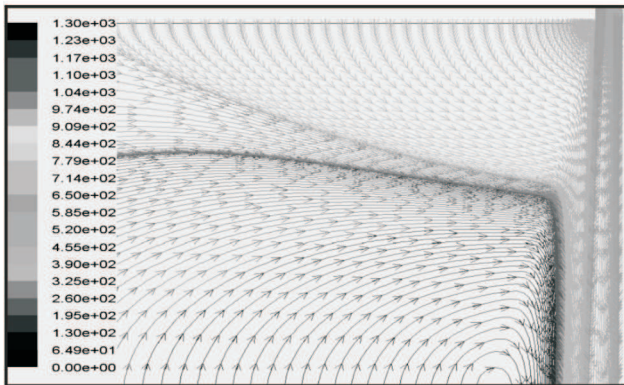


Figure 6: Flow path lines with $\Delta P=0$ Pa

After applying $\Delta P=0.1$ Pa, figure 7 shows that there is no more recirculation in the jet.

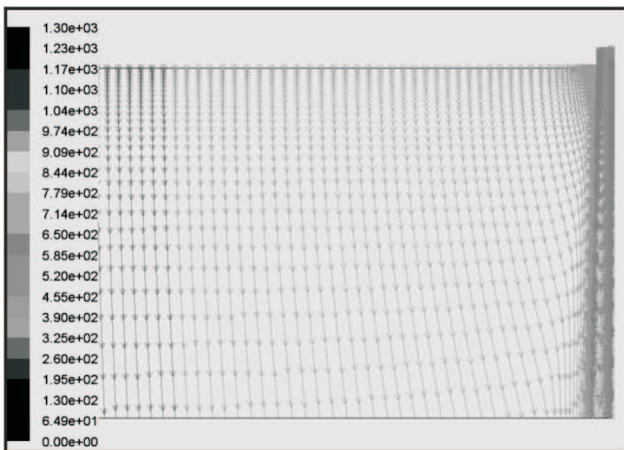


Figure 7: Flow path lines with $\Delta P=0.1$ Pa

3.2. MESH

Two types of meshes were generated i.e. Coarse Mesh and Fine mesh by using commercial software

GAMBIT.

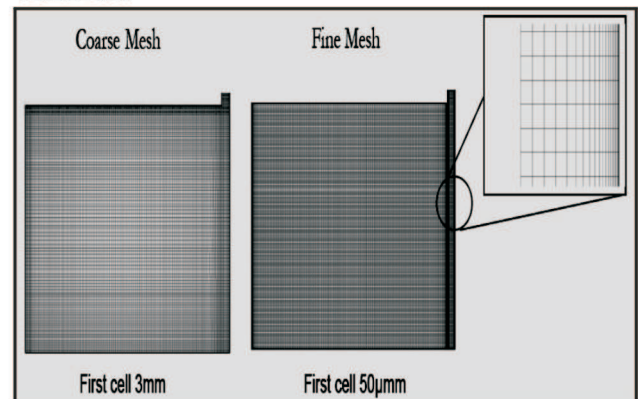


Figure 8: Mesh types used for the 2D wall jet configuration

Coarse mesh was generated to obtain global information of the expected results, while the Fine mesh was generated to obtain specific and detailed information. Coarse mesh was generated by using first cell 3 mm, and total number of cells is 15230, the fine mesh for 4cm nozzle width configuration was generated first cell as 50µm and total number of cells are 38904, and for the fine mesh using 2cm nozzle width configuration mesh was generated by using first cell as 50 µm first cell and total number of cells are 89000. The meshes are shown in the figure 8. To validate these meshes it is very important to calculate Y^+ at wall, to confirm either it respects the numerical recommendations or not, which is shown in the figure (9 a) and (9b). In figure 9a we can observe that the value of Y^+ increases with respect to distance from 2.5 to 36 maximum while for the coarse mesh it is affordable up to 100. Similarly while having a look on figure 9b the value of Y^+ increases with respect to distance and it lies between 0.9 and 1.3 maximum while for the fine mesh it is affordable up to 5.

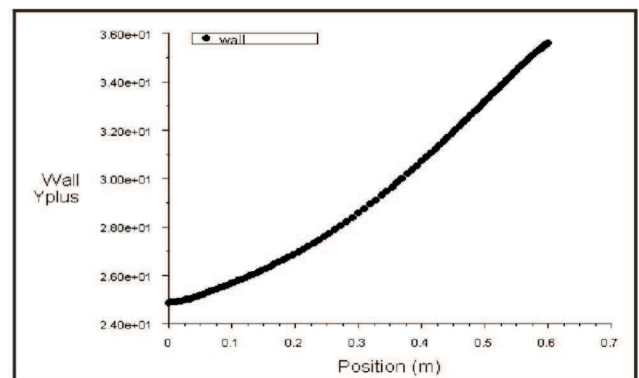


Figure 9a: y plus for coarse mesh

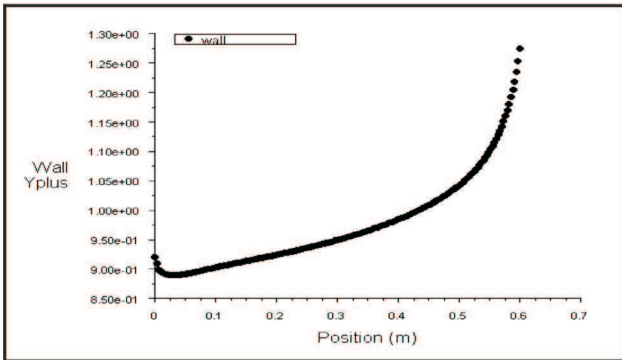


Figure 9b: y plus for fine mesh

3.3. COMPARISONS OF CONFIGURATION HAVING 4 CM NOZZLE WIDTH (COARSE MESH)

3.3.1. MEAN VELOCITY PROFILES (COARSE MESH:)

When the wall jet develops, its velocity is reduced and it expands normal to the wall. The behaviour of maximum velocity (U_m) and half-width (b) is used to investigate the decrease in the velocity and normal expansion to the wall. A good agreement between the mean velocity profiles measured in this work (i.e. both experimentally and numerically) and those obtained by [3] also reported by [18]. The velocity profiles of both configurations (i.e. with nozzle width 4 cm and 2 cm respectively) obtained by FLUENT using six different turbulent models to validate with the LDV results are plotted at different Y-positions. Figure 10a represents velocity profile at y-position = 2.5 cm therefore at an aspect ratio ($Y/b=0.625$) which is just 2.5 cm below the nozzle exit. Rectangular shape velocity profiles are due to a fact that at this point flow is not developed, this location is potential core. Figure 10b illustrates that how jet starts developing and the rectangular shape of velocity profiles begins to change in semi-circular shape. The numerical results are in good agreement with the LDV results, Reynolds shear stress model (RSM) and Standard K-epsilon (SKE), and are much closer to the experimental results than other turbulent models, and give relative error less than 5%. Figure 10c illustrates velocity profiles of developed region and we have obtained almost identical curves of LDV results as well as the numerical results. Figure 10d also shows a good agreement in the curves of numerical and LDV results. The comparison with data in [3] is also made, the difference between data of [3] and our experimental data is due to the difference between aspect ratio. Aspect ratio at this point as $Y/b = 8.625$, while in the [3]

minimum aspect ratio of 21.7 is used. All models seem to be in good agreement with experiments performed using with Laser Doppler Velocimetry (LDV).

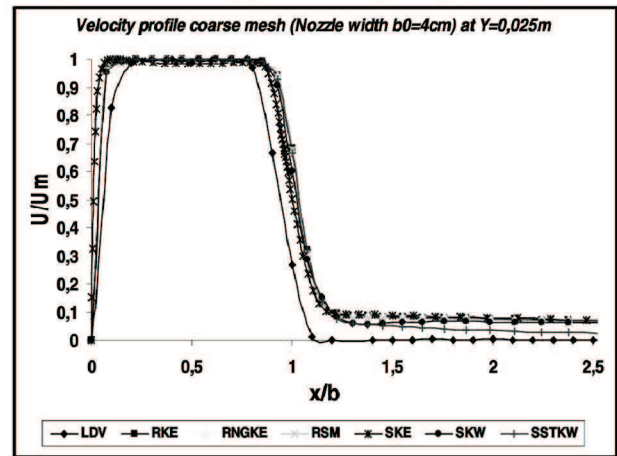


Figure 10a: Velocity profiles at potential core

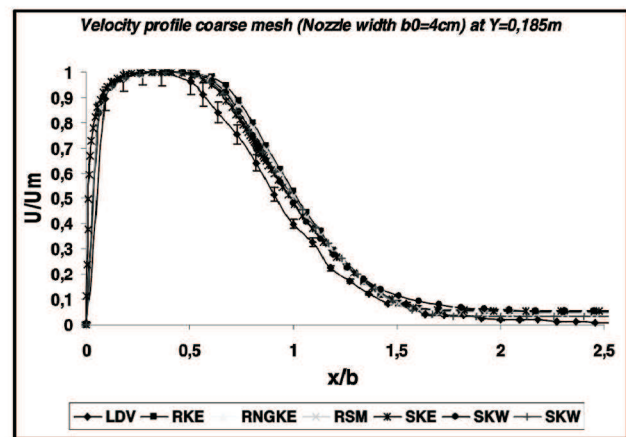


Figure 10b: Velocity profiles (Coarse mesh) at y=18.5 cm

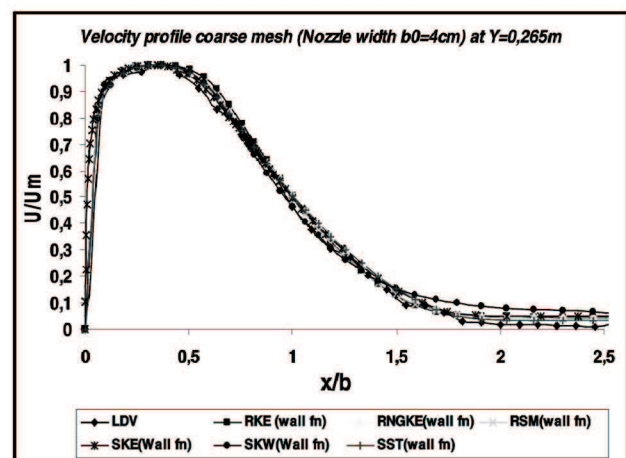


Figure 10c: Velocity profiles (Coarse mesh) at y=26.5 cm

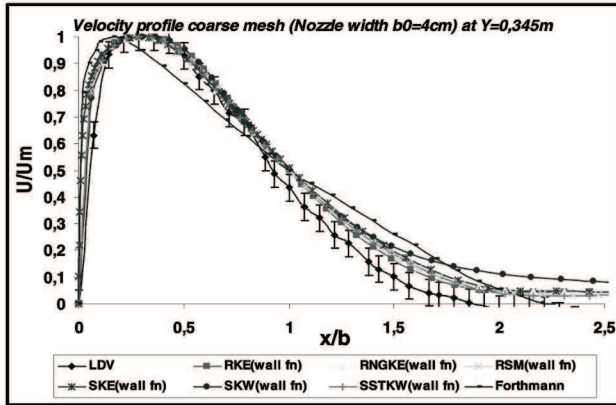


Figure 10d: Velocity profiles (Coarse mesh) at y=34.5cm

3.3.2 MAXIMUM VELOCITY DECAY (COARSE MESH)

Figure 11 illustrates the maximum velocity decay at y-positions. Results are compared with an analytical equation for developed flow which is proposed in [15].

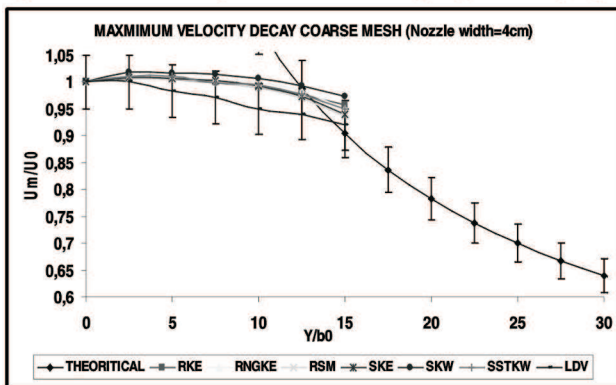


Figure 11: Maximum Velocity decay (Coarse mesh)

$$\frac{U_m}{U_0} = 3.5 / \sqrt{x/b_0} \text{ For } \frac{x}{b_0} \text{ up to } 100 \quad (4)$$

Similarity in curves is observed according to the correlation proposed. However, due to small aspect ratio (y/b) of 15 in our case, it could not be compared for larger aspect ratios. Reynolds shear stress (RSM) and Standard K-Epsilon turbulence models have good agreement with both LDV within five percent of standard deviation.

3.3.3. JET ENTRAINMENT (COARSE MESH):

Jet entrainment is compared with an equation proposed in [18],

$$\frac{Q}{Q_0} = \left[1 + 0.04 \frac{\bar{x}}{b_0} + 0.0046 \left(\frac{\bar{x}}{b_0} \right)^{0.8} \right] \quad (5)$$

In figure 12 both numerical and LDV results show better accordance with the equation. All numerical models show good agreement with the LDV results with 5% of maximum deviation, where Reynolds shear stress model (RSM) is closest to LDV results.

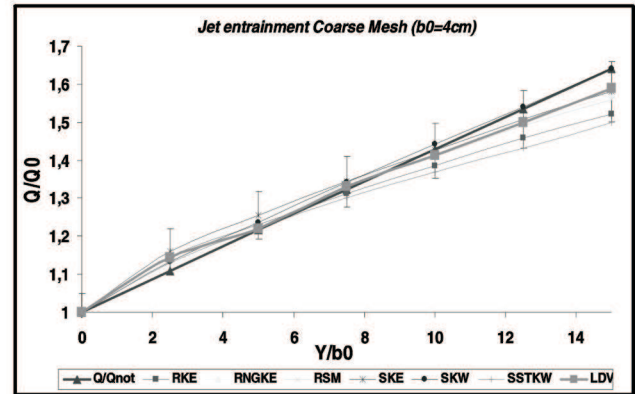


Figure 12: Jet entrainment (Coarse mesh)

Considering the anisotropy of the turbulence, RSM is an appropriate model for predicting the flow structure precisely.

3.3.4. COEFFICIENT OF FRICTION (COARSE MESH):

An equation given by Sigalla (1958) is reported in [15],

$$C_f^u = \frac{\tau_0}{(\rho U_0^2 / 2)} \approx \frac{0.0565}{(Um\delta/\nu)^{1/4}} \quad (6)$$

In figure 13 coefficients of friction obtained numerically are compared with the equation (6); all turbulent models show good agreement with it. It was not possible to determine the coefficient of friction experimentally because with LDV it is not possible to measure velocity at few μm of wall.

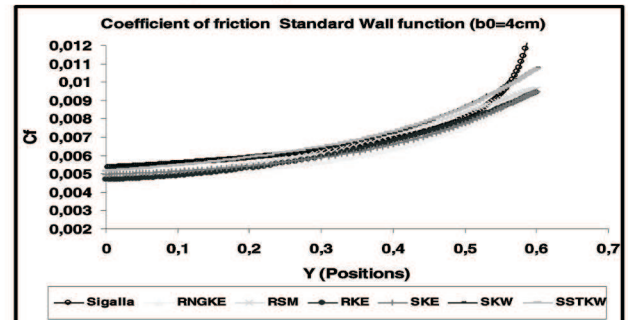


Figure 13: Coefficient of friction (Coarse mesh)

3.4. COMPARISONS OF CONFIGURATION HAVING 4 CM NOZZLE WIDTH (FINE MESH)

3.4.1. MEAN VELOCITY PROFILES (FINE MESH)

Mean velocity profiles are compared for a refined mesh in a similar way as previous. The numerical results are compared with the same LDV results with whom the results were compared for the coarse mesh. Figure 14a presents velocity profile at y -position=0,025, same position on which we have already discussed the coarse mesh case. Good agreement between numerical and experimental results was observed. With a changed mesh some variations were seen in the Standard K-Omega turbulent model, where velocity does not diminish according to experimental and other turbulent models. Figure 14b this velocity profile shows some rectangular and semi-circular mixed shapes, because after the potential core jet starts to develop. At this y -position a good agreement between numerical results and experimental results is also observed, except standard K-Omega. Figure 14c also shows the velocity profile at developed flow. LDV and numerical results coincide with each other, except standard K-Omega which shows some agreement while velocity increases but becomes constant at $U/U_m = 3$. In figure 14d, data given in [3] was also added to see the similarity in curves. As we have already discussed that the difference in profiles is due to large aspect ratio which was used by Förthmann in 1934, otherwise both numerical and experimental results coincide with each other except the standard K-Omega turbulent model.

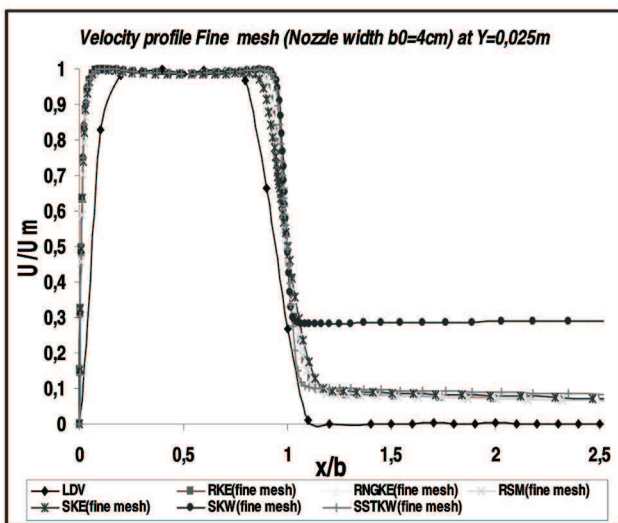


Figure 14 a: Velocity profiles at potential core (Fine mesh)

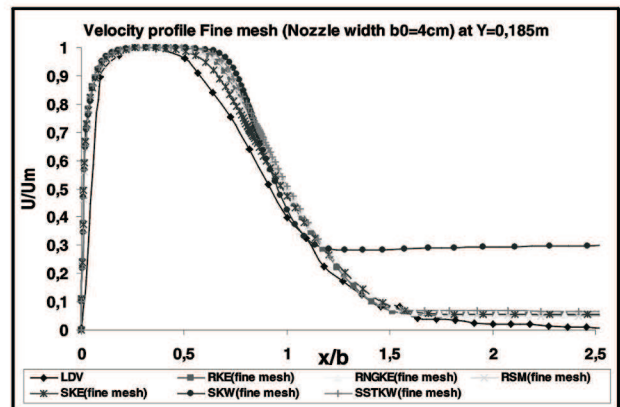


Figure 14b: Velocity profiles (Fine mesh) at $y=18.5$ cm

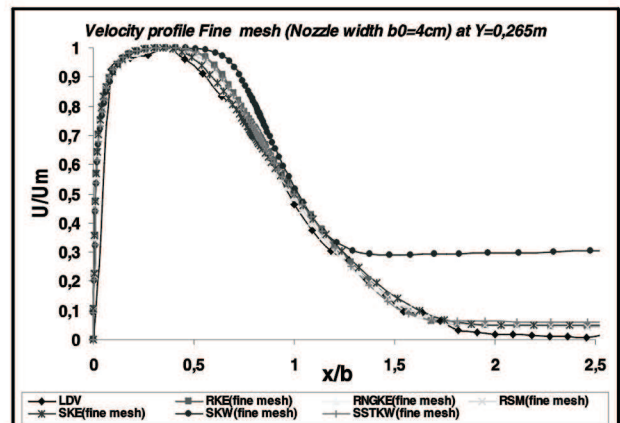


Figure 14c: Velocity profiles (Fine mesh) at $y=26.5$ cm

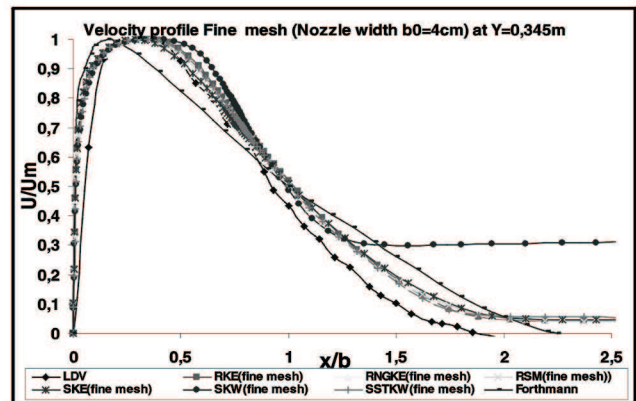


Figure 14d: Velocity profiles (Fine mesh) at $y=34.5$ cm

3.4.2. MAXIMUM VELOCITY DECAY (FINE MESH)

Figure 15, which show a good agreement in maximum velocity decay of experimental and numerical results with equation (4). SKE, RSM and Standard K Omega turbulent models are closer to the LDV results.

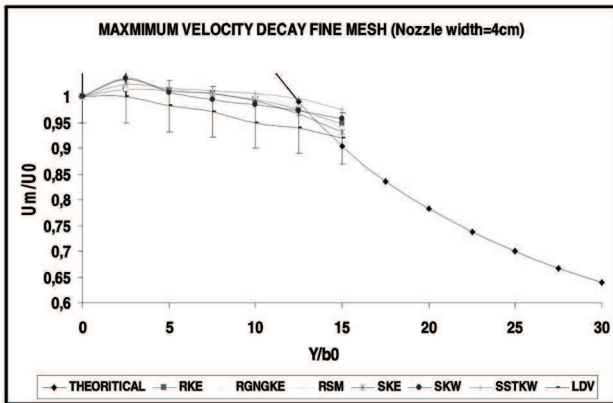


Figure 15: Maximum Velocity decay (Fine mesh)

3.4.3. JET ENTRAINMENT (FINE MESH)

Figure 16 illustrates numerically obtained jet entrainment compared with the equation (5) and LDV results. A good agreement was observed between all turbulent models and LDV results with maximum 5% standard deviation.

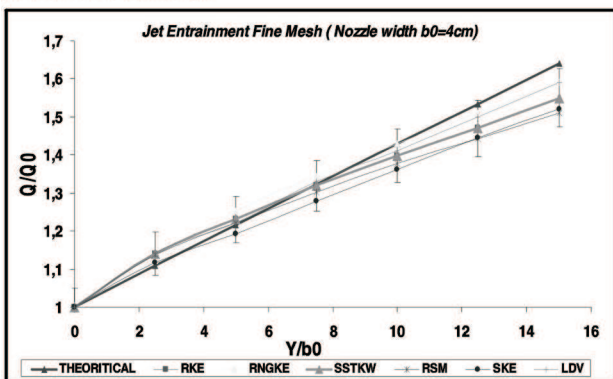


Figure 16: Jet entrainment (Fine mesh)

3.4.4 COEFFICIENT OF FRICTION (FINE MESH):

Figure 17 illustrates the comparison between the equation (6) and numerical curves of coefficient of friction. RSM, RNGKE and SKE turbulent models are much closer to the theoretical curve.

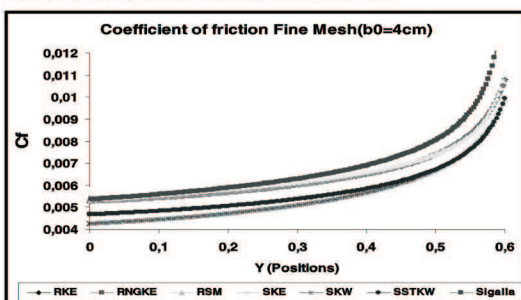


Figure 17: Coefficient of friction (Fine mesh)

3.4.5. Y-PLUS

Velocity distributions in the boundary layer region of plane wall jet are plotted in figure 5.15. This graph is drawn at y-position= 0.3 m, where from $Y^+=10$ the curves obey the log law

$$\frac{U}{U_*} = 5.6 \log\left(\frac{yU_*}{\nu}\right) + 4.9$$

and from $Y^+=1$ to $Y^+=10$ the curves are concave in shape [9] and [10].

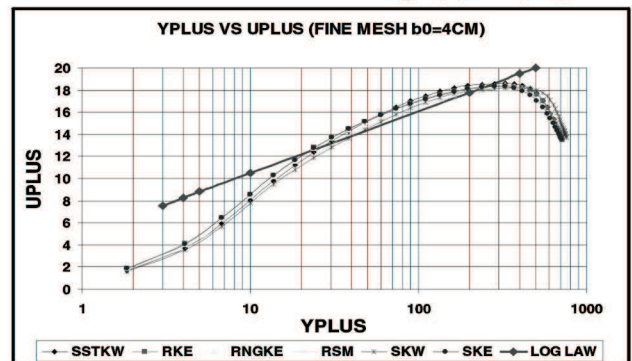


Figure 18: Y^+ Vs U^+ (Fine Mesh nozzle width $b_0= 4cm$)

Turbulent models RSM, SKE are much closer than the other models to the line of log law.

3.5. COMPARISONS OF CONFIGURATION HAVING 2 CM NOZZLE WIDTH (FINE MESH)

3.5.1. MEAN VELOCITY PROFILES:

For the configuration of 2 cm nozzle width the same comparisons were also made. Figure 19 shows behaviour of velocity at y-position=0.345m. This profile is at flow developed region and all turbulent models have shown good agreement with LDV results as well as with data given in [4].

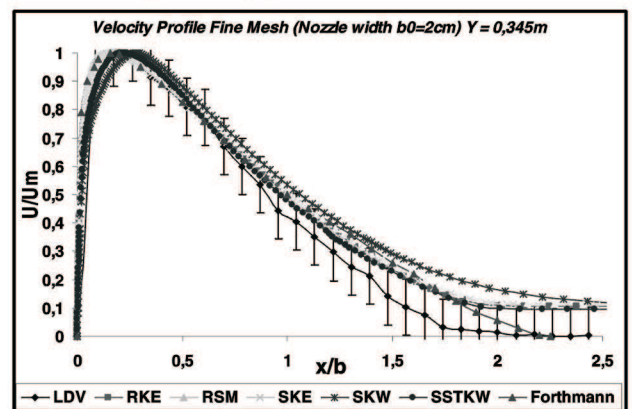


Figure 19: Velocity profiles (Fine mesh $b_0=2cm$) at $y=34.5 cm$

SKE and RSM are closer than the other turbulent models to the LDV results. RSM model improves the prediction of the velocity level in the jet and in some special cases it may influence the entire flow in the occupied zone [2].

3.5.2. MAXIMUM VELOCITY DECAY:

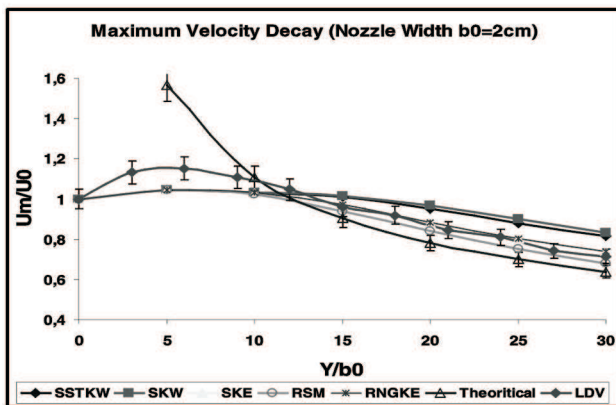


Figure 20: Maximum Velocity decay (Fine Mesh $b_0 = 2\text{cm}$)

Like previous cases, maximum velocity decay curve is found to be in accordance with the equation (4) and LDV results. Figure 20 shows the maximum velocity decay curve of configuration having 2 cm nozzle width. All turbulent models are found to be in good accordance with the equation (4) and LDV curves. LDV curve is between RSM and SKE curves.

3.5.3. JET ENTRAINMENT

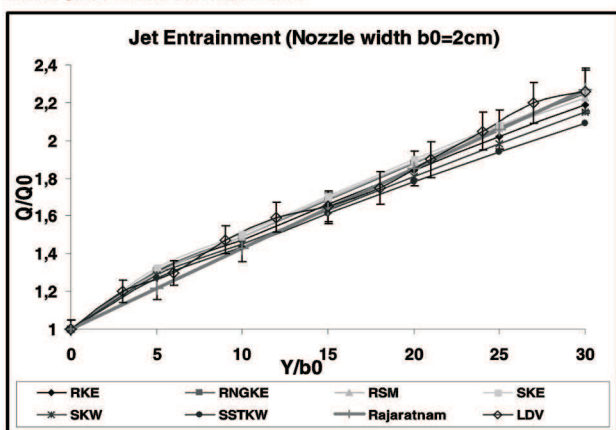


Figure 21: Jet Entrainment (Fine Mesh nozzle width $b_0 = 2\text{cm}$)

Figure 21 illustrates the comparison between equation (5), LDV results and numerical results for the Jet

entrainment. A good agreement was observed between all turbulent models and LDV results with maximum 5% of standard deviation.

3.5.4. COEFFICIENT OF FRICTION:

Figure 22 all turbulent models follow curve of the equation (6) with a slight difference from nozzle exit. This may be due to the fact that all theoretical equations are valid for developed flow regions.

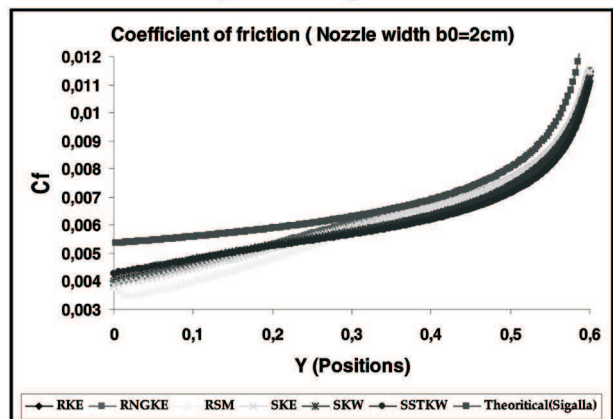


Figure 22: Coefficient of friction (Fine Mesh nozzle width $b_0 = 2\text{cm}$)

RNGKE, RSM and SKE are very close to the theoretical curve in flow developed region.

3.5.5. Y-PLUS

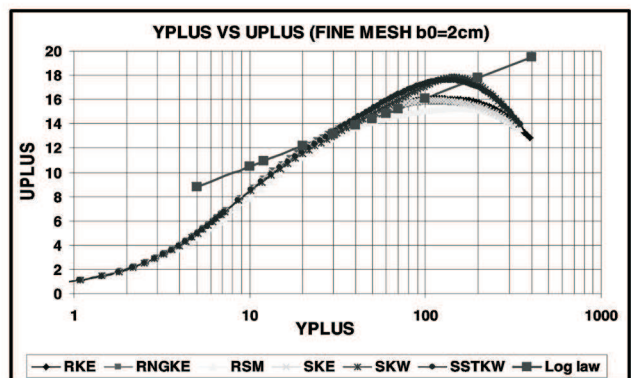


Figure 23: $Y^+ Vs U^+$ (Fine Mesh nozzle width $b_0 = 2\text{cm}$)

Velocity distributions in boundary layer region of plane wall jet are plotted in figure 23. Turbulent models SKW and SSKW are over predicting the log law, while the other four turbulent models have good agreement with the log law line.

4. CONCLUSION AND FUTURE PROSPECTIVE

The study on wall jet was performed on two different configurations of nozzle width 4cm and 2cm respectively. With the obtained results of plane wall jet tested in prototype by using Laser Doppler velocimetry (LDV) and analytical results were used to validate numerical results of turbulent models obtained by using a commercial code FLUENT. A good accordance was obtained between experimental, numerical and analytical results by comparing their velocity profile, maximum velocity decay curves, amount of jet entrainments, coefficients of friction curves and velocity distributions in boundary layer regions. From the numerical point of view it was also concluded that use of fine mesh gives more accurate results than the coarse mesh. As for as turbulent models investigated numerically by using commercial code FLUENT almost found with good agreement with experimental and analytical results. The turbulent models SKE and Reynolds shear stress model (RSM) were in better accordance with the LDV results as compared to other four models.

Experiments are performed to analyze cavity flow with varying degree of cavities resembling vertical display cabinets with LDV and PIV techniques to validate numerical simulations. Moreover this prototype is designed to observe the cross-flow characteristics (which will be tested in near future) applied to RDC. Therefore, another blower will be blown horizontally to see the perturbation behaviour with the vertically blown air, so called air curtain. The objective is to decrease the entrainment rate which is a main factor influencing on refrigeration load. This may be helpful for designing an energy efficient air curtain.

REFERENCES

- [1] AméniMokini, HatimMhiri, Georges Le Palec, Philippe Bournot., (2008) *Numerical study of vertical wall jets*: International Journal of Fluid and Thermal Engineering 1:4 2008.
- [2] A. Schälin and P.V. Nielsen, (2004), Impact of turbulence anisotropy near walls in room airflow, *Indoor Air*14 (2004), pp. 159–168.
- [3] E. Förthmann, Überturbulentestrahlaus breitung, *Ingenieur-Arch*5 (1) (1934), pp. 42–54 translated as: Turbulent jet expansion. National Advisory Committee for Aeronautics, Technical Memorandum, No. 789, National Aeronautics and Space Administration, USA, 1936.
- [4] E. Loth, P. Bhattacharjee., (2004), *Simulations of laminar and transitional cold wall jets*.International Journal of Heat and Fluid Flow 25 (2004) 32–43.
- [5] Georges RIGOT., (2009), *Meubles frigorifiques de vente*, Techniques de l'Ingénieur, traité Génie énergétique, (Institut français du froid industriel IFFI)Cemagref Dossier.
- [6] G. I. Barenblatt, A. J. Chorin, and V. M. Prostokishin; (2005),*The turbulent wall jet: A triple-layered structure and incomplete similarity*
- [7] Hazim B. Awbi., (1991), *Ventilation of Buildings*. Second edition Spon London EC4P 4EE.
- [8] Homayun K. Navaz, Brenda S. Henderson, RaminFaramarzi, Ahmad Pourmovahed, Frederic Taugwalder, (2005), *Jet entrainment rate in air curtain of open refrigerated display cases*. International Journal of Refrigeration 28 :p 267–275.
- [9] <http://www.cfd-online.com>.
- [10] Introductory FLUENT notes, FLUENT v6.3(2006), www.fluentusers.com.
- [11] J.G. Eriksson, R.I. Karlsson, J. Persson., (1998), *An experimental study of a two-dimensional plane turbulent wall jet*. Experiments in Fluids Volume 25, p 50-60.
- [12] Ke-zhi Yu, Guo-liang Ding ,Tian-ji Chen, (2007),*Simulation of air curtains for vertical display cases with a two-fluid model*.Applied Thermal Engineering 27 (2007) 2583–2591.
- [13] M. Amin, H.K. Navaz, D. Dabiri& R. Faramarzi, (2006), *Air curtains of open refrigerated display cases revisited: a new technique for infiltration ratemeasurements*.
- [14] MitoubkietaTapsoba., (2005), *Thèse Etudes expérimentale et numérique de l'aéraulique dans un véhicule frigorifique*. Thèse à l'Institut de recherche pour l'ingénierie de l'agriculture et de l'environnement; Unité de recherche Génie des procédés frigorifiques- Antony- France.
- [15] Rajaratnam, N., (1976), *Turbulent jets*: Elsevier Publishing Co.
- [16] Rajaratnam, N. and Subramanya, K., (1967), *Diffusion of rectangular wall jets in wider channels*. J. Hydraul. Res., 5:281-294.
- [17] S.S Aloysius, L.C Wrobel., (2009), *Comparison of flow and Dispersion properties of free and wall turbulent jets for source dynamics characterisation*.Environmental Modelling& Software 24 (2009), p 926–937.